

Symmetric Conditions for Strain Analysis in a Long Thick Cylinder under Internal Pressure Using NASIR Unstructured GFVM Solver

S.R. Sabbagh-Yazdi¹⁾, M. Esmaili²⁾ and M.T. Alkhamis³⁾

¹⁾ Associate Professor, KN Toosi University of Technology, Civil Engineering Department (Iran)

²⁾ M.Sc. Graduate, KN Toosi University of Technology, Civil Engineering Department (Iran)

³⁾ Assistant Professor, Civil Engineering Department, College of Technological Studies (Kuwait)
malkhamis@hotmail.com (Corresponding Author)

ABSTRACT

Utilization of symmetric condition in NASIR Galerkin Finite Volume Method for linear triangular element unstructured meshes is introduced for numerical solution of two dimensional strain and stress fields in a long thick cylinder section. The developed shape function free Galerkin Finite Volume structural solver explicitly computes stresses and displacements in Cartesian coordinate directions for the two- dimensional solid mechanic problems under either static or dynamic loads. The accuracy of the introduced algorithm is assessed by comparison of computed results of a thick cylinder under internal fluid pressure load with analytical solutions. The performance of the solver for taking advantage of symmetric conditions is presented by computation of stress and strain contours on a half and a quarter of the cylinder section.

KEYWORDS: Symmetric condition, Unstructured finite volume method, Unstructured linear triangular element, Strain-stress solver, Thick cylinders.

INTRODUCTION

Computation of strain and stress fields in the section of a long cylinder which is subjected to internal or external pressure requires two-dimensional plane strain analysis. On the other hand, proper numerical algorithm facilitates computational modeling of such a structural element with normal pressure on its curved boundaries. For the cases that the use of symmetric boundaries is considered, the algorithm should be able to handle specific boundary conditions (i.e., inclined sliding supports).

Among the wide variety of numerical methods which have been proposed for the numerical solution of partial differential equations, Finite Element Method

(FEM) has firmly established itself as the standard approach for problems in Computational Solid Mechanics (CSM), especially with regard to deformation problems involving non-linear material analysis (Lv et al., 2007; Zienkiewicz et al., 1989).

It is well known that numerical analysis of solids in incompressible limit could lead to difficulties. For example, fully integrated displacement based lower-order finite elements suffer from volumetric locking, which usually accompanies pressure oscillation in incompressible limit (Bijelonja et al., 2006). Also, there are some difficulties for producing stiffness matrix and shape function in order to increase the convergence rate.

Although certain restrictions on mesh configuration had to be imposed to avoid locking, these restrictions were less severe than those of the equivalent FEM meshes.

The FVM has been developed from early finite difference techniques and has similarly established itself within the field of Computational Fluid Dynamics (CFD) (Slone et al., 2003; Bailey et al., 1999; Lv et al., 2007). However, similar to FEM, FVM integrates governing equation(s) over pre-defined control volumes (Zienkiewicz et al., 1989), which are associated with the elements making up the domain of interest and, therefore, preserve the conservation properties of the equations. Although, the Finite Volume Method (FVM) was originally developed for fluid flow and heat and mass transfer calculations (Slone et al., 2003) recently, it has been generalized for stress analysis in isotropic linear and non-linear solid bodies. Therefore, the interest in FVM application to the structural analysis problems involving incompressible materials has grown during the recent years. From the results of several benchmark solutions, the FVM appeared to offer a number of advantages over equivalent finite element models. For instance, it can be stated that, unlike FDM solution, FVM solution is conservative and incompressibility is exactly satisfied for each discretized sub-domain (control volume) of the computational domain (Bailey et al., 1999).

In principle, because of the local conservation properties, the FVMs should be in a good position to solve such problems effectively. Furthermore, numerical calculation with meshes consisting of triangular cells showed excellent agreement with analytical results. Meshes consisting of quadrilateral FVM cells displayed too stiff behavior, indicating a locking phenomenon (Demirdzic and Martinovic, 1999). Therefore, researchers have applied FVMs to problems in CSM over the past decade (Slone et al., 2003; Sabbagh-Yazdi et al., 2003) and it is now possible to classify these methods into two approaches; cell-centered ones and vertex-based ones.

In the previous work of the authors, the *NASIR* Unstructured Galerkin Finite Volume Method structural solver was introduced and applied for analysis of two-dimensional strain and stress fields in a thick cylinder (in a form of a complete ring) with internal fluid

pressure (Timoshenko and Goodier, 1982). Considering symmetric may provide considerable computational work load. However, implementation of proper symmetric boundary conditions (i.e., sliding supports in cut sections) is necessary for such a technique.

In this paper, the explicit approach introduced is based on Galerkin approach with a kind of matrix free vertex base FVM on unstructured meshes of linear triangular elements. The accuracy of the introduced method is assessed by comparison of computed stresses and displacements for a thick cylinder with internal fluid pressure load with analytical solutions and the performance of the solver is demonstrated in terms of stress and strain contours as well as convergence behavior of the method to the steady state condition. Finally, the use of symmetric boundary conditions for reducing computational work load (without degradation of the accuracy of the results) is examined.

MATHEMATICAL MODEL

The governing equation for force equilibrium of any continuum in the absence of body forces is given by the following general form of Cauchy equation:

$$\rho \frac{\partial^2 u_i}{\partial t^2} = \frac{\partial \sigma_{ij}}{\partial x_j} \quad (j = 1, 2) \quad (1)$$

Here, ρ is the material density and u_i is the displacement in the i direction. Considering direction $i=1$ as x and $i=2$ as y , stresses are defined as:

$$\begin{aligned} \sigma_{xx} &= \left(C_1 \frac{\partial u_x}{\partial x} + C_2 \frac{\partial u_y}{\partial y} \right) \\ \sigma_{xy} = \sigma_{yx} &= C_3 \left(\frac{\partial u_x}{\partial y} + \frac{\partial u_y}{\partial x} \right) \\ \sigma_{yy} &= \left(C_2 \frac{\partial u_x}{\partial x} + C_1 \frac{\partial u_y}{\partial y} \right) \end{aligned} \quad (2)$$

For plane strain problems:

$$\begin{aligned} C_1 &= \frac{E(1-\nu)}{(1+\nu)(1-2\nu)}, \\ C_2 &= \frac{E\nu}{(1+\nu)(1-2\nu)}, \\ C_3 &= \frac{E}{2(1+\nu)} \end{aligned} \quad (3)$$

In which E is the elastic modulus and ν is the Poisson's ratio.

NUMERICAL FORMULATION

Following the Galerkin Finite Element Method for discretization of the spatial derivatives of the governing equation on a sub-domain Ω consisting of linear triangular elements (Figure 1), after multiplying the residual of the above equation by the linear shape function φ of node n and integrating over the sub-domain, the weak form of the governing equation may be written as:

$$\int_{\Omega} \varphi_n \rho \frac{\partial^2 u_i}{\partial t^2} d\Omega = - \int_{\Omega} (\bar{F}_i \cdot \bar{\nabla} \varphi_n) d\Omega + [\varphi_n \cdot \bar{F}_i]_{\gamma} \quad (4)$$

Here, the stress vector is defined as $\bar{F}_i = \sigma_{ij} \hat{i} + \sigma_{i2} \hat{j}$.

It should be noted that since the shape function φ_n is equal to unity at node n and zero at the γ boundary of sub-domain Ω , the last boundary term of the above equation vanishes for the internal sub-domains.

Using the Finite Difference Method for discretization of the time derivative of i direction displacements, the shape function free Galerkin Finite Volume Method form the above equation can be formulated as (Lv et al., 2007):

$$u_i^{t+\Delta t} = 2u_i^t - u_i^{t-\Delta t} + \frac{3(\Delta t)^2}{2\rho\Omega_n} \sum_{k=1}^N (\tilde{\sigma}_{i1}\Delta y - \tilde{\sigma}_{i2}\Delta x)_k \quad (5)$$

In the above formulation, the stresses can be computed as (Lv et al., 2007):

$$\begin{aligned} \tilde{\sigma}_{xx} &\approx \left\{ \frac{1}{A_k} \sum_{m=1}^3 (C_1 u_x \Delta y - C_2 u_y \Delta x)_m \right\} \\ \tilde{\sigma}_{xy} = \tilde{\sigma}_{yx} &\approx \left\{ \frac{1}{A_k} \sum_{m=1}^3 (C_3 u_x \Delta y - C_3 u_y \Delta x)_m \right\} \\ \tilde{\sigma}_{yy} &\approx \left\{ \frac{1}{A_k} \sum_{m=1}^3 (C_2 u_x \Delta y - C_1 u_y \Delta x)_m \right\} \end{aligned} \quad (6)$$

where A_k is the area of triangular element (with

$m=3$ sides) associated with boundary side k of the sub-domain Ω_n (Figure 1).

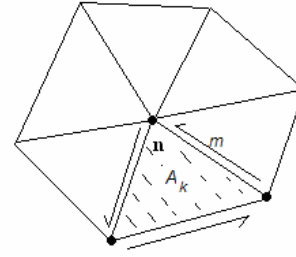


Figure 1: A sub-domain Ω_n formed by linear triangular elements meeting a node n

COMPUTATIONAL STEPPING

Note worthy is that the above formulation can be solved via explicit iterations without any matrix manipulations, considering proper limit computational step Δt . The time step Δt_n for each control volume can be computed as (Lv et al., 2007):

$$\Delta t_n \leq \frac{r_n}{\sqrt{E/\rho(1-\nu^2)}} \quad (7)$$

Here, r_n is the average radius of equivalent circle that matches with the desired control volume ($r_n = \Omega_n / P_n$). For any control volume n

($\Omega_n = \sum_{k=1}^{N_{edge}} (\bar{y}\Delta x)_k$), the perimeter can be computed using surrounding edges

$$(P_n = \sum_{k=1}^{N_{edge}} (\Delta l)_k).$$

Due to the variations in sizes of unstructured control volumes' calculations, the allowable time step for the solution of dynamic problems for the entire mesh is limited to the minimum time associated with the smallest control volume of the domain. However, the large variation in grid size for the unstructured mesh will slow down the computations.

In the present work, the local time step of each control volume is used for the computation of static

problems. In this technique, to accelerate the convergence to steady state conditions, the computation of each control volume can advance using a pseudo time step which is calculated for its own control volume. The use of local time stepping greatly enhances the convergence rate.

COMPUTATIONAL RESULTS

In this section, the computational results of stress and strain analysis of a thick cylinder under internal fluid pressure are presented. The numerical solution is performed by the application of Galerkin finite volume method on an unstructured triangular mesh. The analytical solution is used to verify the results and satisfaction equality obtained. The model specifications are illustrated in Table 1.

In the present computation, it is assumed that the cylinder is considerably long, and thus the plane strain assumption is valid. For such a condition, radius stresses and tangential stresses from analytical solution are computed by following relations:

$$\sigma_r = C_1 - \frac{C_2}{r^2} \tag{8}$$

$$\sigma_t = C_1 + \frac{C_2}{r^2} \tag{9}$$

where r is the radius and C_1 and C_2 are two coefficients which can be calculated by using the following relations:

$$C_1 = \frac{p_i r_i^2 - p_o r_o^2}{r_o^2 - r_i^2} \tag{10}$$

$$C_2 = \frac{(p_i - p_o) r_i^2 r_o^2}{r_o^2 - r_i^2} \tag{11}$$

Here p_i and r_i are the interior pressure and interior radius, respectively; and p_o and r_o are the outer pressure and outer radius, respectively.

In order to properly impose the pressure load on a thick cylinder section (complete ring), the unit normal

vectors at boundary nodes are utilized, see Figure 2. The schematic diagram views a thick steel cylinder with 12 kPa interior fluid pressure and zero outer pressure.

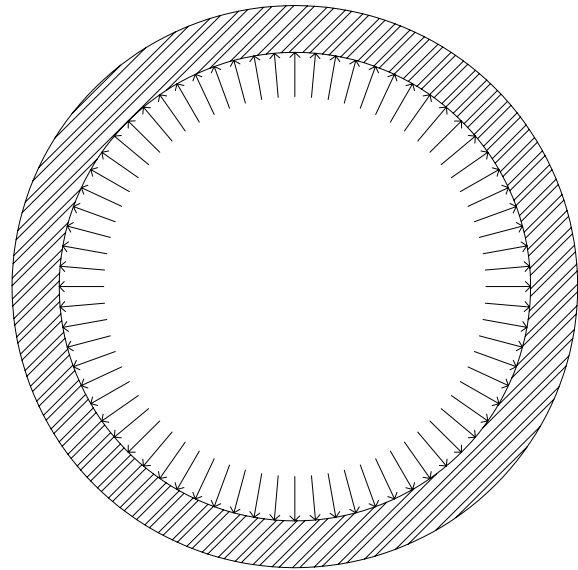


Figure 2: Thick steel under internal pressure

The properties of the cylinder material are tabulated in Table 1.

Table 1: Specifications of a thick cylinder

Parameter	Value
Young's modulus, E	21 MPa
Density, ρ	7850 kg/m ³
Poisson's ratio, ν	0.25
Interior radius	0.5
Outer radius	0.6
Interior pressure	12000 Pa

For Galerkin Finite Volume Method solution of this case, first an unstructured mesh of linear triangular cells is used (Figure 3).

The history of computed maximum displacement is plotted in Figure 4. CPU time consumed for the computations of this case (100,000 iterations) was measured as 51.51 seconds on a P4 computer. This value presents the light computational work load of the described computational solid mechanic algorithm.

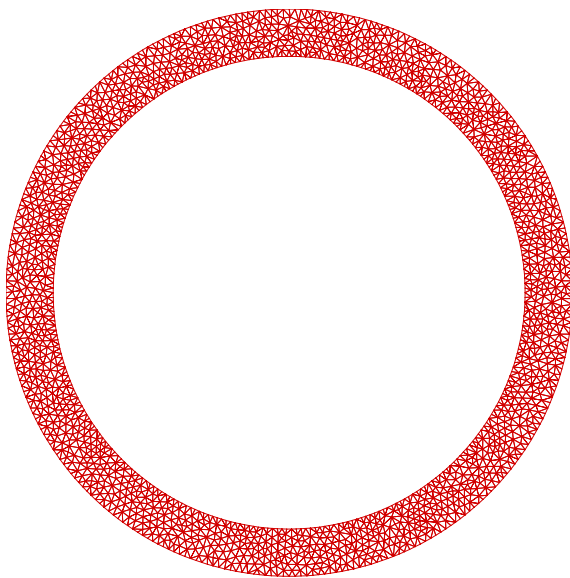


Figure 3: Unstructured computational mesh

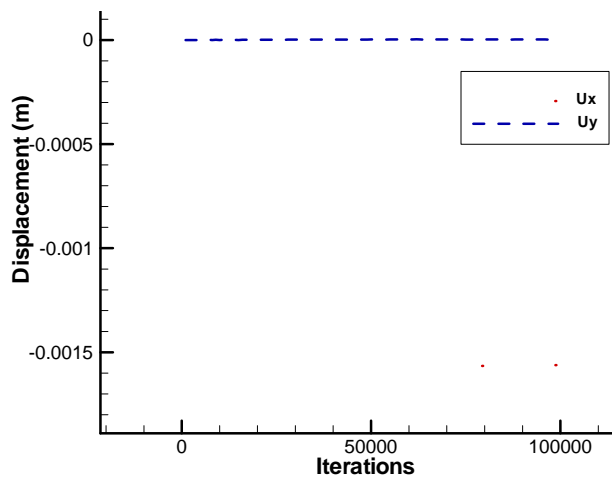
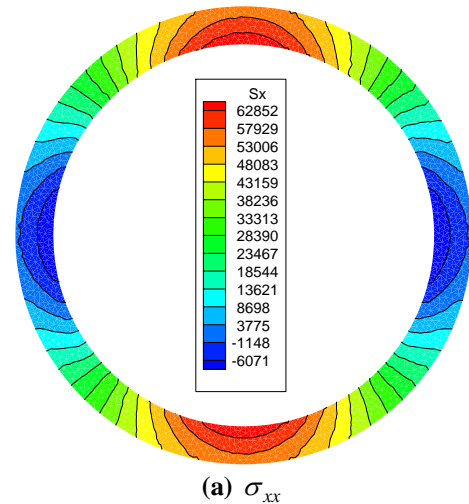
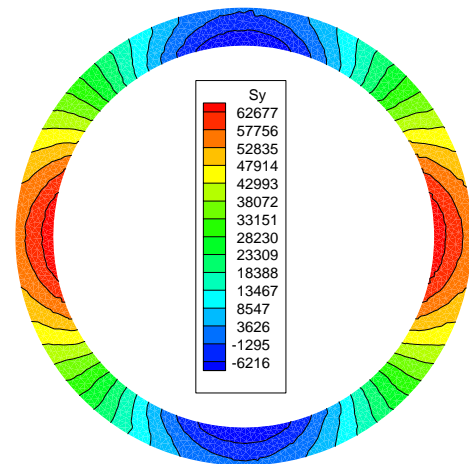


Figure 4: The history of computed maximum displacement

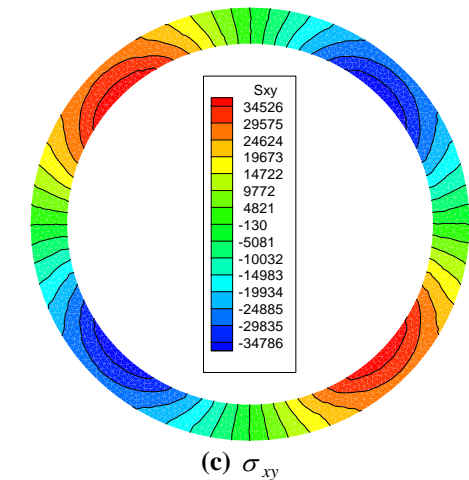
The computed normal and shear stresses for a complete ring present smooth and symmetric contours (Figure 5). The computed results of radial and circumferential stresses are compared with the analytical solution along the thickness of the case (Figure 6). As can be seen, the computed radial and circumferential stresses show good agreement with the exact solution of the case.



(a) σ_{xx}



(b) σ_{yy}



(c) σ_{xy}

Figure 5: Color coded maps of computed results for complete ring (Pa)

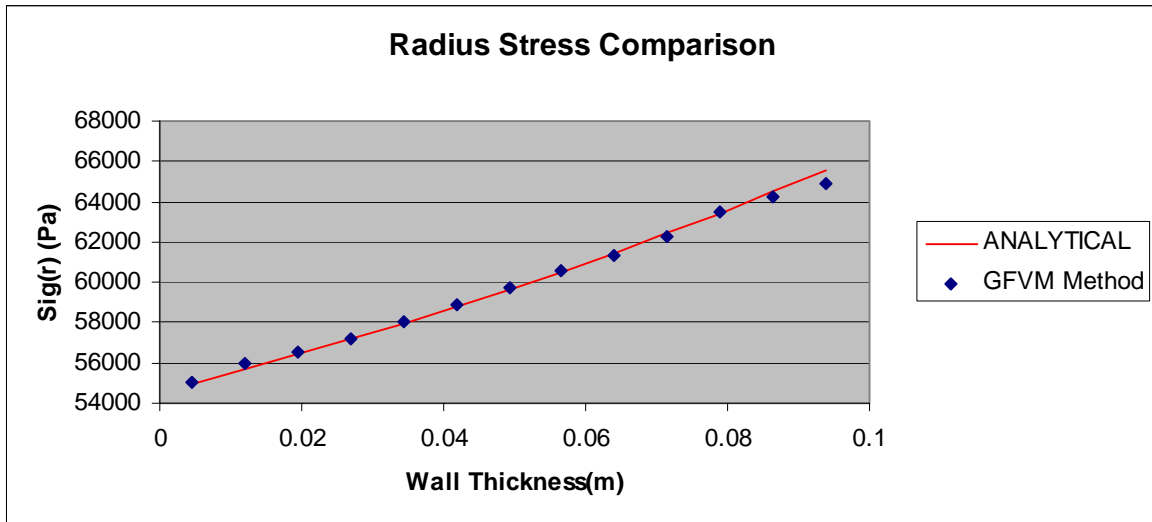


Figure 6: Radial stress compared with the analytical solution along the thickness

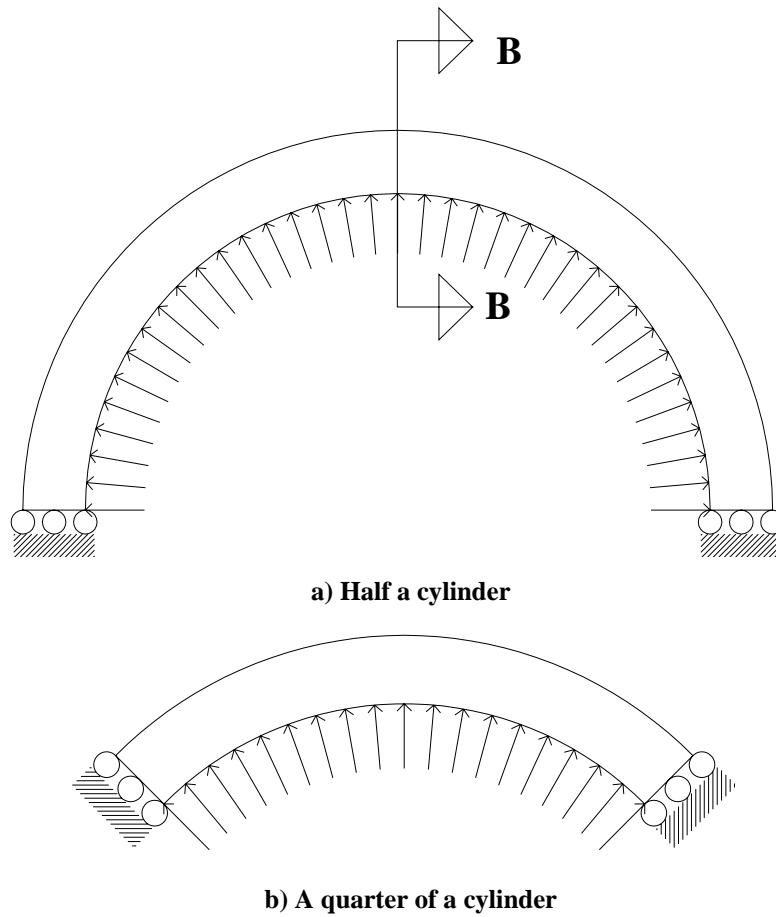
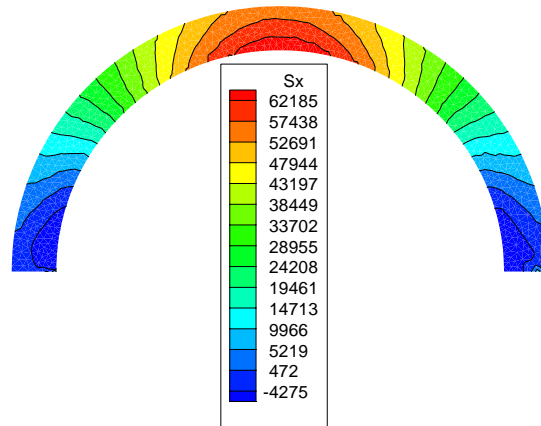
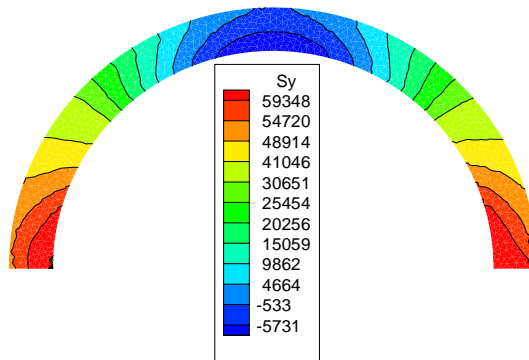


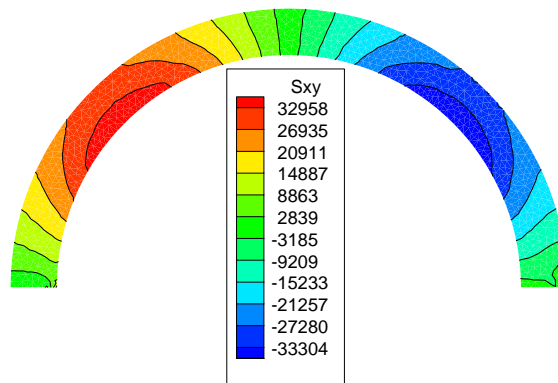
Figure 7: Various symmetric boundary conditions and equivalent sliding supports



(a) σ_{xx}



(b) σ_{yy}



(c) σ_{xy}

Figure 8: Color coded maps of computed results for a half of a ring (Pa)

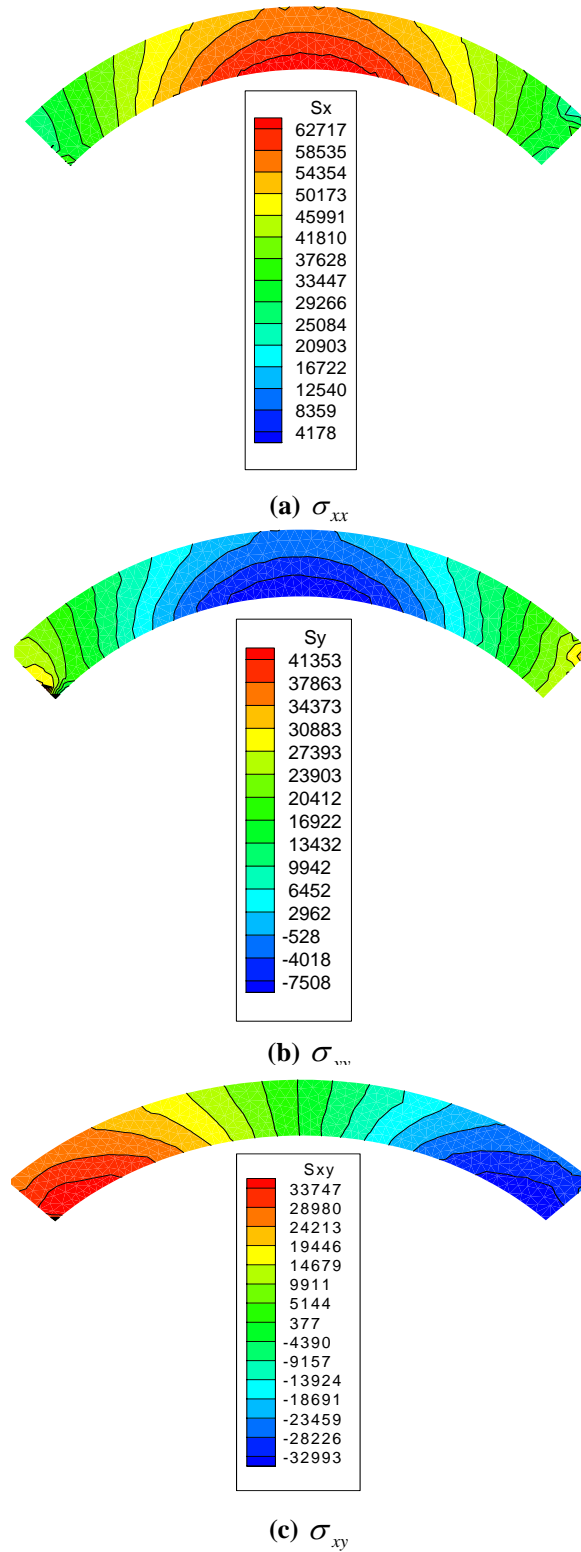


Figure 9: Color coded maps of computed results for a quarter of a cylinder (Pa)

Table 2: Accuracy of the results

Parameter	GFVM solution	Analytical solution	Error
σ_r	66574	66545	0.0436%
σ_t	-11961	-12000	0.32%

Table 3: Error for thick cylinder under internal pressure

Cylinder portion	Stress (Pa)	GFVM solution	Analytical solution	Error (%)
Complete	σ_r	66574	66545	0.0436
Half	σ_r	66685.8	66545	0.21
Quarter	σ_r	67010	66545	0.7

The accuracy of computed radial and circumferential stresses is compared with that of the analytical solution (Table 2). As can be seen from the table, the computed results present minor percentages of error in radial and circumferential stresses.

In the next stage of this work, the use of symmetric boundary conditions by the application of sliding supports and the effects on the accuracy of the results are examined. Figures (7-9) show schematic views of the applied symmetric boundary conditions.

In order to impose the symmetric boundary conditions (sliding supports) for a half and a quarter of the ring, displacements normal to the symmetric boundary are put to zero. The stress contours computed by imposing the symmetric boundary conditions for a half and a quarter of the cylinder are plotted (Figure 8 and Figure 9). As can be seen from the tabulated values in the error report (Table 3), the implementation of symmetric conditions reduces the computational effort with acceptable errors.

REFERENCES

Bailey, C., Taylor, G.A., Cross, M. and Chow, P. 1999.

CONCLUSION

The vertex base explicit matrix free Galerkin Finite Volume Method for the solution of two-dimensional Cauchy equations on an unstructured mesh of triangular elements is described and applied in this paper. Since there is no interpolation function in the numerical formulation of the present solver, the fine meshes provide more accurate results than the coarse ones.

The present model is examined for stress-strain in a thick cylinder under fluid pressure. The comparison of the computed results with the analytical solution presents a promising agreement between the computed results for a complete thick cylinder section and the analytical solution of the case.

Furthermore, the use of symmetric conditions (modeling a half and a quarter of the cylinder section) provides similar results due to efficiency of the developed numerical model as well as proper sliding (symmetric) boundary conditions. This technique provides considerable saving in the computational work load.

Discretization procedures for multi-physics phenomena, *Journal of Computational and Applied Mathematics*, 103: 3-17.

- Bijelonja, I., Demirdzic, I. and Muzaferiya, S. 2006. A finite volume method for incompressible linear elasticity, *Journal of Mechanical Engineering*, 195: 6378-6390.
- Demirdzic, I. and Martinovic, D. 1999. Finite volume method for thermo-elasto-plastic stress analysis, *Computer Methods in Applied Mechanics and Engineering*, 109: 331-349.
- Ly, X., Zhao, Y., Huang, X.Y., Xia, G.H. and Su, X.H. 2007. A matrix-free implicit unstructured multi-grid finite volume method for simulating structural dynamics and fluid–structure interaction, *Journal of Computational Physics*, 225 (1): 120-144.
- Sabbagh-Yazdi, S.R., Alkhamis, M.T., Esmaili, M. and Mastorakis, N.E. 2008. Finite volume analysis of two-dimensional strain in a thick pipe with internal fluid pressure, *International Journal of Mathematical Models and Methods in Applied Sciences*, 1 (2): 162-167.
- Slone, A.K., Bailey, C. and Cross, M. 2003. Dynamic solid mechanics using finite volume methods, Old Royal Naval College, University of Greenwich, *Applied Mathematical Modeling*, 27: 69-87.
- Timoshenko, S.P., and Goodier, J.N. 1982. Theory of Elasticity, McGraw-Hill, New York.
- Zienkiewicz, O.C. and Taylor, R.L. 1989. The Finite Element Method Basic Formulation and Linear Problems, Vol. 1, McGraw-Hill, Maidenhead, UK.